Submitted to the Proc. of the 194th Electrochemical Society Meeting, Lithium Battery Volume, Boston, Nov.1-5, 1998.

BNL-66159

IN SITU X-RAY DIFFRACTION STUDIES OF $Li_xMn_2O_4$ CATHODE MATERIALS BY SYNCHROTRON X-RAY RADIATION

X. Q. Yang, X. Sun, S. J. Lee, and J. McBreen
Brookhaven National Laboratory, Upton, NY 11973

S. Mukerjee
Department of Chemistry, Northeastern University, Boston, MA 02115-5000

M. L. Daroux and X. K. Xing
Gould Electronics Inc., Eastlake, OH 44095-4001

ABSTRACT

In Situ x-ray diffraction studies on $Li_xMn_2O_4$ spinel cathode materials during charge-discharge cycles were carried out by using a synchrotron as x-ray source. Lithium rich (x=1.03-1.06) spinel materials obtained from two different sources were studied. Three cubic phases with different lattice constants were observed during charge-discharge cycles in all the samples when a sufficiently low charge-discharge rate (C/10) was used. There are two regions of two-phase coexistence between these three phases, indicating that both phase transitions are first order. The separation of the Bragg peaks representing these three phases varies from sample to sample and also depends on the charge-discharge rate. These results show that the de-intercalation of lithium in lithium-rich spinel cathode materials proceeds through a series of phase transitions from a lithium-rich phase to a lithium-poor phase and finally to a λ-MnO_2 like cubic phase, rather than through a continuous lattice constant contraction in a single phase.

INTRODUCTION

$Li_xMn_2O_4$ spinel is one of the most promising cathode materials for lithium rechargeable batteries because of its low cost and toxicity. Recent studies have been focused on the problem of capacity fading of this material during cycling, especially at elevated temperature. This fading has been attributed into two sources, the dissolution of Mn^{2+} into the non-aqueous electrolytes (1) and the inhomogeneity of the spinel local structure (2,3) Early ex situ x-ray diffraction studies of $Li_xMn_2O_4$ were performed by Ohzuku et al.(4) They found that two cubic phases coexist for $0.60 > x > 0.27$, and a single cubic phase is present for $1.0 > x > 0.6$. Xia and Yoshio (5) reported in their studies that the two-phase coexistence was suppressed in cathode materials which were prepared "lithium rich" (x=1.04) or "oxygen rich". They also claimed that the two-phase coexistence is one of the key factors for the capacity fading during cycling. By suppressing this phase transition, the capacity fading of the lithium rich cathode materials was significantly improved at the expense of lower initial capacity. In their later XRD studies (6) an in situ technique was used, and the same conclusion that there was a one phase structure for lithium rich spinel was presented. This interesting work raised an important issue: the relationship between the

structural change and the capacity fading of these spinel materials during cycling. However, there are experimental data published by other research groups that show two-phase coexistence in lithium rich spinels. For example, Richard, Koetschou, and Dahn(7) have reported on their in situ XRD studies with the observation of two phase coexistence in the $0.60 > x > 0.27$ range for $Li_xMn_2O_4$ material, where the x value before charge was similar to that in the studies of reference 5 (x=1.02 vs x=1.04). The main difference between these two studies is the charge rate. (C/40 in reference 7 vs C/3 in reference 5). The first issue we want to address in this paper is whether the two phase coexistence region is really being suppressed or not in lithium rich spinel. The second issue we want to address is whether the spinel is a two-phase or a three-phase system during lithium de-intercalation and determine the order of the phase transitions. This issue was raised after Liu, Kowal, and Farrington(8) recently published their in situ XRD and neutron diffraction studies on spinel materials. A new phase diagram for $Li_xMn_2O_4$ during discharge was proposed: from single phase A ($0<x<0.2$) to a two-phase coexistence region A+B ($0.2<x<0.4$), to a single phase B ($0.45<x<0.55$) and finally to a single phase C ($0.55<x<1$). This three-phase model is quite interesting and different from the two-phase system proposed by Ozhuku in reference 4. Since no two-phase coexistence region was observed between phase B and phase C in Liu's study, they claim that the phase transition between B and C is second order. In this letter, experimental evidence will be presented for the first time to show that the three-phase model is correct but that both phase transitions are first order. The unique technique used in this in situ study was the utilization of the synchrotron radiation as x-ray source. By using this technique, we were able to probe the cathode bulk in the transmission mode. Therefore, more detailed structural changes during lithium de-intercalation and intercalation were observed. The effects of charge-discharge rate on the structural change behavior of these spinel materials are also discussed in this paper.

EXPERIMENTAL

Sample A, $Li_xMn_2O_4$ (x=1.05) powder was obtained from Gould Electronics Inc., and sample B, $Li_xMn_2O_4$ (x=1.03-1.06), was purchased from EM Industries Inc.. Cathodes were prepared by slurrying $Li_xMn_2O_4$ powder with 10% PVDF (KynarFlex 2801, Atochem), and 10% acetylene black (w/w) in a fugitive solvent, then coating the mix onto Al foil. After vacuum drying at 100 °C, the electrode disks (2.8 cm^2) were punched and weighed. The average weight of active material was 20mg. The electrodes were incorporated into cells with a Li foil negative electrode, a Celgard separator and a 1 M $LiPF_6$ electrolyte in a 1:1:3 PC:EC:DMC solvent (LP 10 from EM Industries Inc.). Mylar windows instead of beryllium windows were used in these in situ cells.

In situ XRD spectra were collected on beam line X18A at National Synchrotron Light Source (NSLS) were operated at an energy of 10375 eV (λ=1.195 Å). The experimental setup was basically the same as described in our previous paper (9).

RESULTS AND DISCUSSION

DISCLAIMER

DISCLAIMER

Portions of this document may be illegible in electronic image products. Images are produced from the best available original document.

Fig.1 shows the in situ XRD spectra of sample A, $Li_xMn_2O_4$ (x=1.05) during the first charge from 3.5V to 4.5V under constant current condition at C/6 rate. The x value was assigned to each scan based on the assumption that x value decreased uniformly from 1.05 to 0 during the charging process. The missing data towards the end of charge was due to the unavailability of the x-ray beam. Since the charging process was continued during this period, the incomplete data were kept in the plot to give correct indication of the charge states. All the in situ spectra in this paper are treated in the same way. Since the cubic structure of $Li_xMn_2O_4$ spinel is well known (space group Fd3m), only three Bragg peaks, (511), (440), and (531) were recorded for each 2θ scan (32 min for each scan). From the spectra in Fig. 1, only one cubic phase can be clearly identified with all three peaks moving to higher angles in a continuous fashion during charge. The calculated lattice constant of the cubic unit cell, based on the position of (531) peak, contracted from 8.25 Å for the uncharged cell to 8.07 Å for the fully charged cell. This is in good agreement with the results reported by Xia and Yoshio(5,6). However, because a slower charge rate (C/6 vs C/3) and an in situ technique was used in this study, more detailed structural changes were recorded in Fig.1. All three peaks start broadening when the cell was charged to x=0.41, and become narrower at x=0.09. This is an indication of a two-phase coexistence and a phase transition in this region. In order to record more spectra during discharge, the data collecting time for each 2θ scan was reduced from 32 min to 16 min while the discharge rate was kept the same at the C/6 rate. The results are plotted in Fig. 2. Although the signal to noise ratio of the spectra was not as good as in Fig.1 due to the shorter data collecting time, clear phase transitions were observed through the spectra in Fig.2. During discharge, starting from x=0.20, a set of new peaks appeared at lower angles and grew in intensity at the expense of the intensity of the original peaks. At x=0.60, the third set of peaks emerged and finally became the dominant peaks at the end of discharge. It is quite clear from the spectra in Fig. 2 that the cathode material went through distinguishable phases during discharge. However, from scan at x=0.30 to x=0.85, all the Bragg peaks are quite broad and not very well resolved, indicating the non-equilibrium state of the system. We then decide to study this sample with a slower charge-discharge rate. In order to eliminate any unpredictable factors introduced by the cycling history of the first cell, a fresh cell was constructed for the slower charge-discharge rate studies. The cathode disk used in the second cell was punched from the same batch as the first cell. The charge rate was reduced from C/6 to C/10. Fig. 3 is a plot of the charging curve of this cell. This is a typical charging curve for $Li_xMn_2O_4$ spinel with two plateaus. This curve was divided into five regions based on the two plateaus. From x= 1.05 to x=0.95, the curve is a steep slope, this region is assigned to a single phase I. From x=0.95 to x=0.55, the first plateau around 4.05V is attributed to a phase I + phase II coexistence region. From x=0.55 to x=0.44, the curve is the step between the two plateaus, this region is assigned to a single phase II. From x=0.44 to x=0.06, the second plateau around 4.15V is attributed to the phase II + phase III coexistence region. From x=0.06 to x=0, the steep slope region is assigned to a single phase III. The in situ XRD patterns collected with 32 min per scan are plotted in Fig.4. All three phases observed in Fig.2 are clearly resolved in Fig.4. At x=0.90, all three peaks start getting broader. With the decreasing value of x, the three peaks become more and more broad. Clear peak separation can be observed in scans with x=0.60 and x=0.55. The new peaks representing the third phase emerged in the scan with x=0.40. They become the dominating peaks at the end of charge in the scan with x=0.05. For this lithium rich spinel cathode material sample

A, three cubic phases with different lattice constants can be clearly identified during charge. In order to simplify the discussion, we will refer them as phase I (a=8.25 to a=8.20Å), phase II (a=8.17 Å to a=8.12 Å), and phase III (a=8.05 Å). Unlike the clear peak separation in scans with x=0.20 and x=0.15, the peak separation in scans with x=0.55 and x=0.50 is rather small and could easily be missed if the charge rate is too high. Comparing the phase diagram based on the shape of charging curve in figure 3 and the phase separation observed in figure 4, the I +II region and II + III region matched very well. However, from x=0.55 to x=0.4, rather than observing the single phase II as expected, both phase I and phase II are observed in figure 4. This inconsistency between the XRD data and the charging curve is due to the non-equilibrium state of the system caused by fast charging rate. This retardation effect is more pronounced in Fig 2 where the charge rate is even faster. The voltage measured in the charging curve is determined by the composition of cathode at the electrolyte-cathode interface, that can be quite different to the bulk when the charging rate is high. The XRD spectra during discharge (C/10 rate) for the same battery cell are plotted in Fig.5. The data collecting time for each 2θ scan is 32 min. The reversible transitions from phase III to phase II and then from phase II to phase I are confirmed. However, the peak separation is not as clear as in Fig. 4 for charging.

$Li_xMn_2O_4$ spinel samples obtained from other commercial sources such as Sedema Division of Sadacem and EM Industries Inc. were also studied. All of them showed the same three phase behavior during charge-discharge cycle if a sufficiently slow charge-discharge rate was used. Due to the limited space, here we only present the results of sample purchased from EM Industries Inc., which we named as sample B. This sample B is also a lithium rich $Li_xMn_2O_4$ (x=1.03-1.06) spinel material. The results of samples from other sources will be discussed in later publications. The in situ XRD spectra of sample B during the first charge are plotted in Fig. 6. The data collection time was 32 min for each 2θ scan and the charge rate was C/10. The phase transition from phase I to phase II is not as clear as in Fig. 4 for sample A. The phase II to phase III transition is more obvious through peak broadening at x=0.25 and x=0.20, but no clear peak separation was observed. The in situ XRD spectra of sample B in the same cell during the first discharge are plotted in Fig. 7. The data collecting time was 32 min for each 2θ scan and the discharge rate was C/10. All the three phases observed in Fig.5 can be identified in Fig. 7. Clear peak separations are observed at x=0.32 in the phase III and phase II coexistence region. On the other hand, the phase II and phase I coexistence region is recognizable through the peak broadening which is more obvious than in fig. 6 for charging.

As discussed in the introduction, one important issue we want to address in this paper is the structural change behavior of the lithium rich samples. For this purpose, both sample A and sample B used in this study are lithium rich. As demonstrated by the spectra in figure 1, when a fast charge rate was used, the phase transitions were masked. Since the charging rate used in reference 5 is even faster (C/3), it may have masked the phase transition and led the authors to conclude that the phase transition was suppressed in lithium rich samples. However, when slower charge rates were used in this study, clear phase transitions were observed in our lithium rich samples. We would also like to point out that even when the same rate was used for both charge and discharge, the peak separations in figure 4 for charge are much clearer than in figure 5 for discharge. This tells us that many other factors, such as the electrochemical history of the cell, the nucleation of the new crystal phase, and

the original crystal grain size of the samples, all have significant effects on the XRD spectra. Based on our results on lithium rich samples obtained from two different sources, we believe that the phase transitions are not suppressed in lithium rich samples. Therefore, the relationship between the capacity fading and the phase transition also needs to be reevaluated.

The phase diagram of $Li_xMn_2O_4$ spinel material in figure 4 of this paper, derived from the in situ XRD spectra, is different from the two-phase model. The two phase model was first proposed by Ohzuku (4) and widely accepted by most research groups in this field. We would like to point out that the three-phase model was first proposed by Liu, Kowal, and Farrington (8). However, the ex situ XRD technique used in reference 8 was not able to resolve the two-phase coexistence region between phase I and phase II (phase C and phase B in reference 8). Therefore, this transition was mistakenly assigned as second order phase transition and the two- phase coexistence region was mistakenly assigned as single phase C. From Fig.2, Fig. 4, Fig.5, Fig.6, and Fig. 7 in this paper, a clear two-phase coexistence region of phase I and phase II was observed. Therefore, we conclude that the transition between them is a first order phase transition. The three-phase model presented in this paper is also in good agreement with the results of cyclic voltammetry studies(10) which concluded that a two step de-intercalation process was responsible for the two oxidation peaks during charge. We would also like to point out that although the phase I to phase II transition and two-phase coexistence region have not been recognized before, their existence was hinted at in several published papers. For example, "a small discontinuous gap of *ca.* 0.02 A is observed" around x=0.55 in reference 5. The same gap was also observed in reference 8. In reference 7, a low angle Bragg reflection was attributed to the "presence of some disconnected grains of material which are not available for intercalation". However, in comparing to our data, we believe that this reflection is the result of a residue of phase I.

All the three phases of $Li_xMn_2O_4$ spinel observed in this study have the same cubic structure. The only distinguishable feature is the difference in lattice constant, which was observed through the peak separation in XRD spectra. However, the lattice constant of phase I and phase II also changes during charge-discharge, which makes it difficult to identify the phase transitions. From Fig. 1 and Fig. 4, we see the important effect of charge rate. When high charge rate was used, the non-equilibrium state of the system increased the lattice constant range of phase I and phase II, and resulted in the spectra in Fig. 1, which looks like a continuous lattice constant change with just one phase. When a slower charge rate was used, the spectra in Fig 4 show clear peak separations. Since the lattice constant of phase III is almost fixed, the phase transition from phase II to phase III is easier to observe. On the other hand, the overlapping of lattice constant ranges of phase I and phase II during fast charge-discharge make it difficult to distinguish them from each other. The effect of charge rate on the non-equilibrium states is one of the important results from this study.

CONCLUSION

Based on in situ XRD spectra at different charge and discharge rates, a three-phase model is proposed for lithium rich $Li_xMn_2O_4$ spinels as an intrinsic feature during lithium

intercalation and de-intercalation. The phase diagram based on the charging curve matched very well with the phase transitions observed through the XRD spectra. The charge-discharge rate has significant effects on the XRD spectra during charge-discharge.

ACKNOWLEDGMENT

This work was supported by the U. S. Department of Energy Division of Materials Science of the Office of Basic Energy Sciences, and the Office of Energy Research, Laboratory Technology Research Program, Under Contract No. DE-AC02-98CH10886.

REFERENCES

1. J. M. Tarascon, F. Coowar, G. Amatuci, F. K. Shokoohi, and D. G. Guyomard, *J. Power Sources*, **54**, 103 (1995)
2. S. Bach, M. Henry, N. Baffier, and F. K. Shokoohi, *J. Solid State Chem.*, **88**, 325 (1990)
3. P. Barboux, J. M. Tarascon, and F. K. Shokoohi, *J. Solid State Chem.*, **94**, 185 (1991)
4. T. Ohzuku, M. Kitagawa, and T. Hirai, *J. Electrochem. Society*, **137**, 769 (1990)
5. Y. Xia and M. Yoshio, *J. Electrochem. Society*, **143**, 825 (1996)
6. Y. Xia Y. Zhou, and M. Yoshio, *J. Electrochem. Society*, **144**, 2593 (1997)
7. M. N. Richard, I. Keotschau, and J. R. Dahn, *J. Electrochem. Society*, **144**, 554 (1997)
8. W. Liu, K. Kowal, and G. C. Farrington, *J. Electrochem. Society*, **145**, 459 (1998)
9. S. Mukerjee, T. R. Thurston, N. M. Jisrawi, X. Q. Yang, J. McBreen, M. L. Daroux, and X. K. Xing, *J. Electrochem. Society*, **145**, 466 (1998).
10. J. M. Tarascon, W. R. McKinnon, F. Coowar, T. N. Bowmer, G. Amatucci, and D. Guyomard, *J. Electrochem. Society*, **141**, 1421 (1994).

Key words: X-ray diffraction, Cathode materials, Lithium battery.

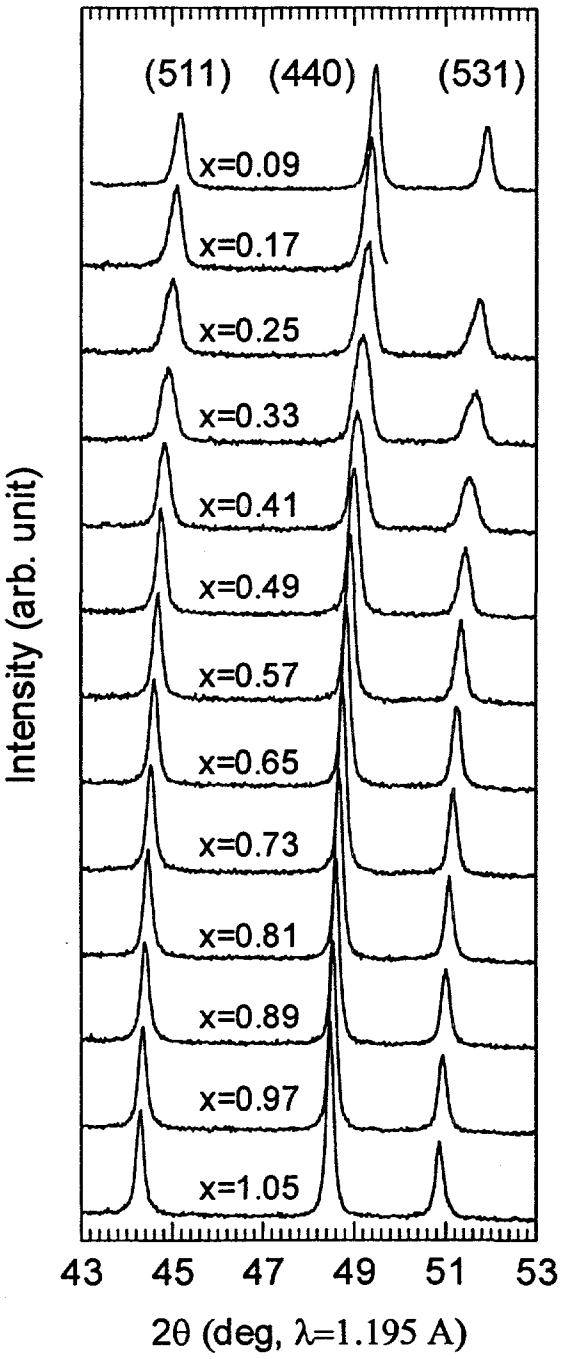

Figure 1. In situ XRD patterns of $Li_xMn_2O_4$ sample A during first charge with C/6 rate, 32 min for each scan.

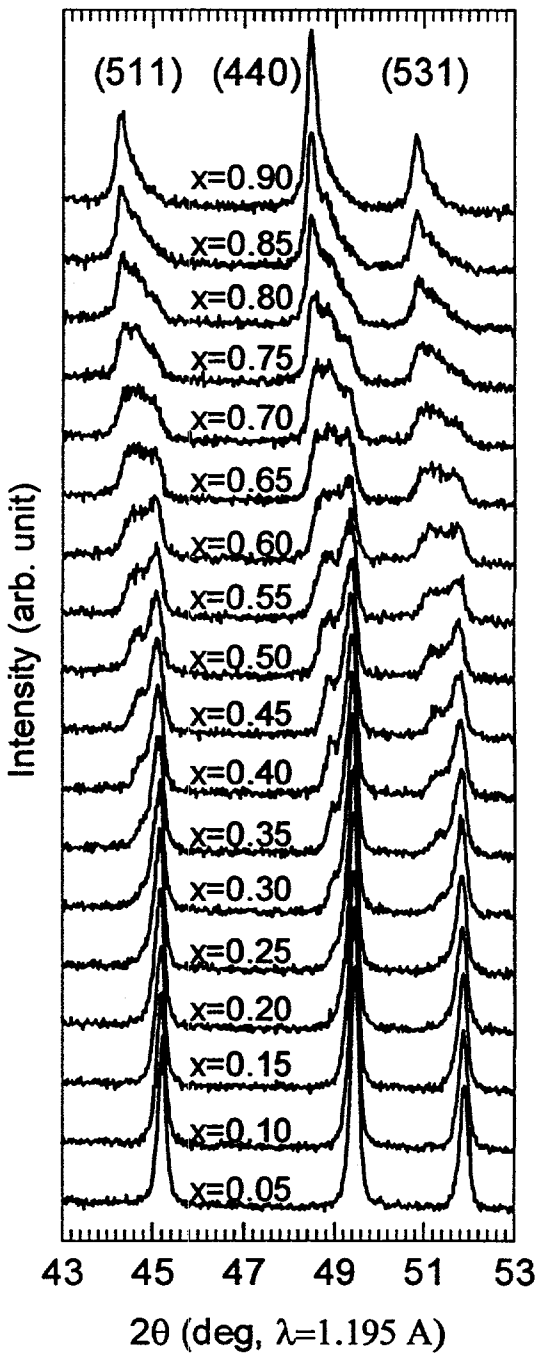

Figure 2. In situ XRD patterns of $Li_xMn_2O_4$ sample A during first discharge with C/6 rate, 32 min for each scan.

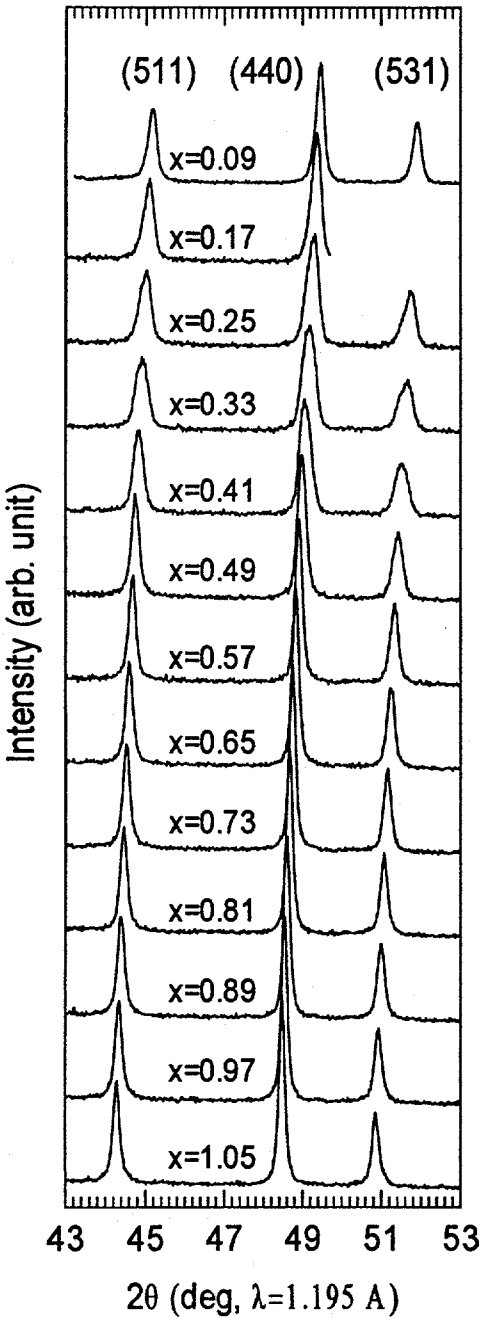

Figure 1. In situ XRD patterns of $Li_xMn_2O_4$ sample A during first charge with C/6 rate, 32 min for each scan.

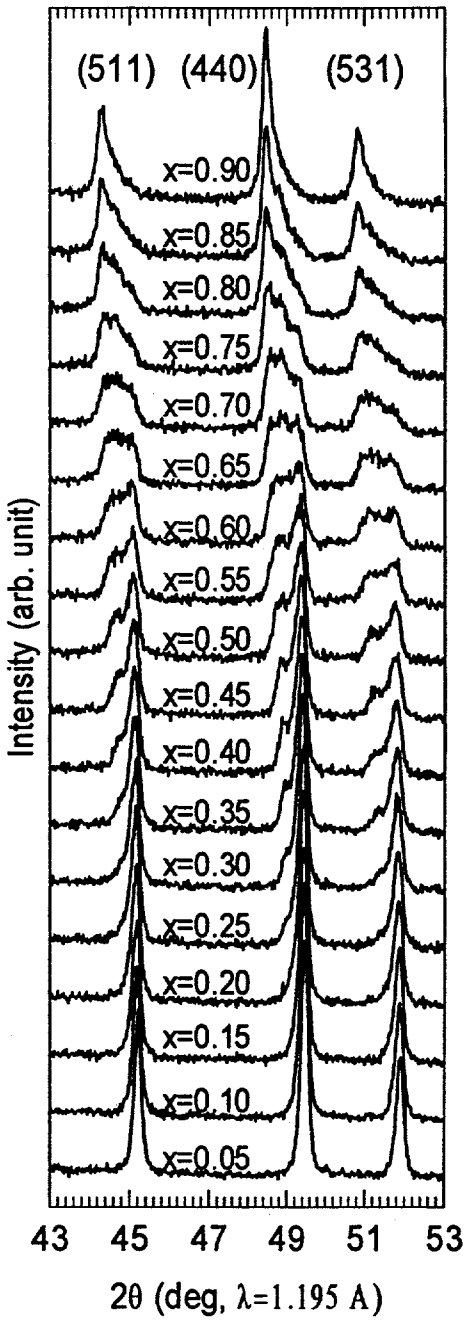

Figure 2. In situ XRD patterns of $Li_xMn_2O_4$ sample A during first discharge with C/6 rate, 32 min for each scan.

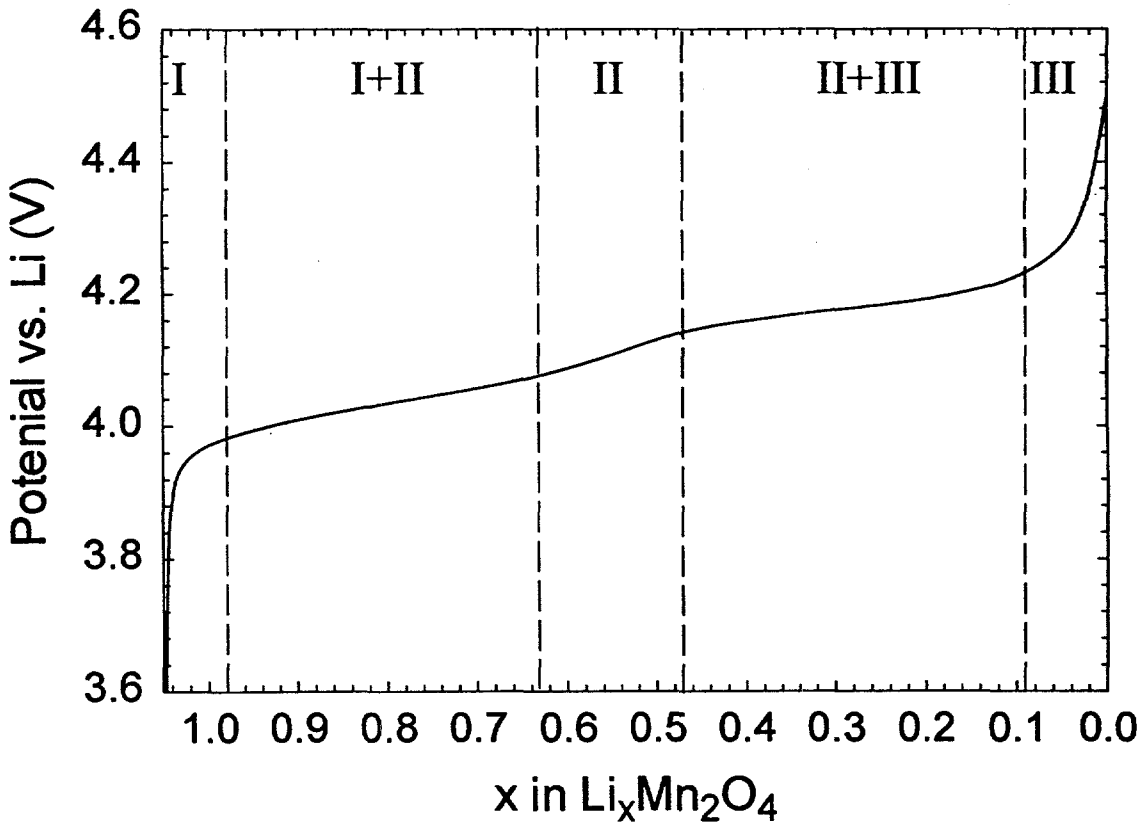

Figure 3. The first charge curve of $Li/Li_xMn_2O_4$ cell using sample A as cathode with C/10 rate.

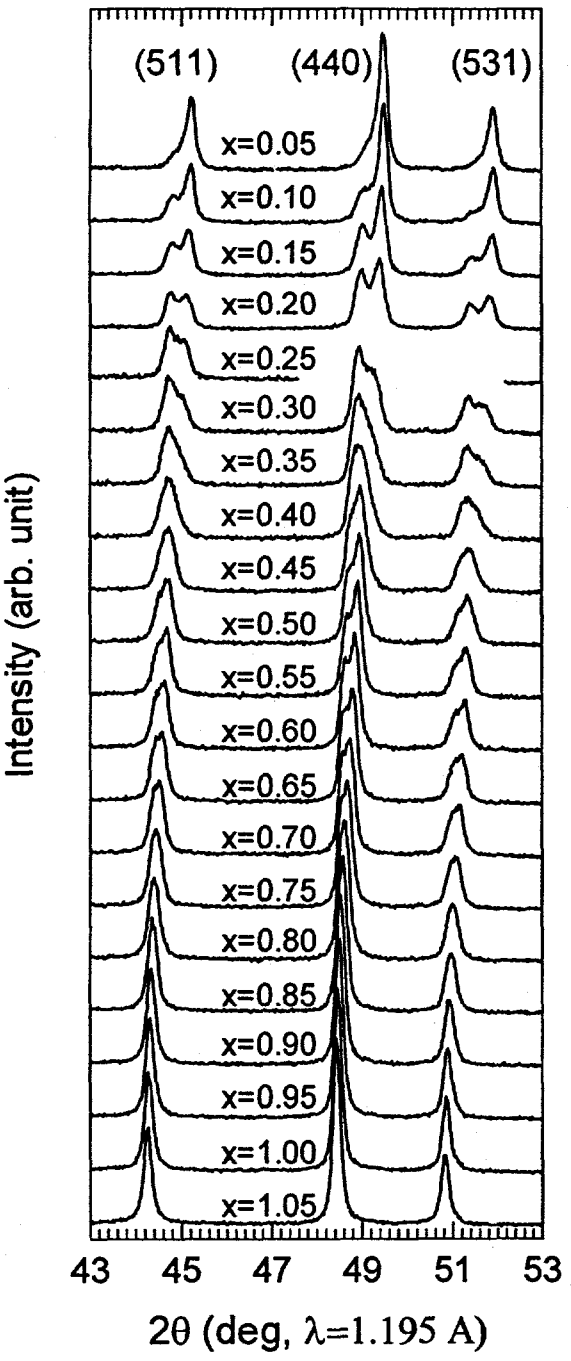

Figure 4. In situ XRD patterns of $Li_xMn_2O_4$ sample A during first charge with C/10 rate, 32 min for each scan.

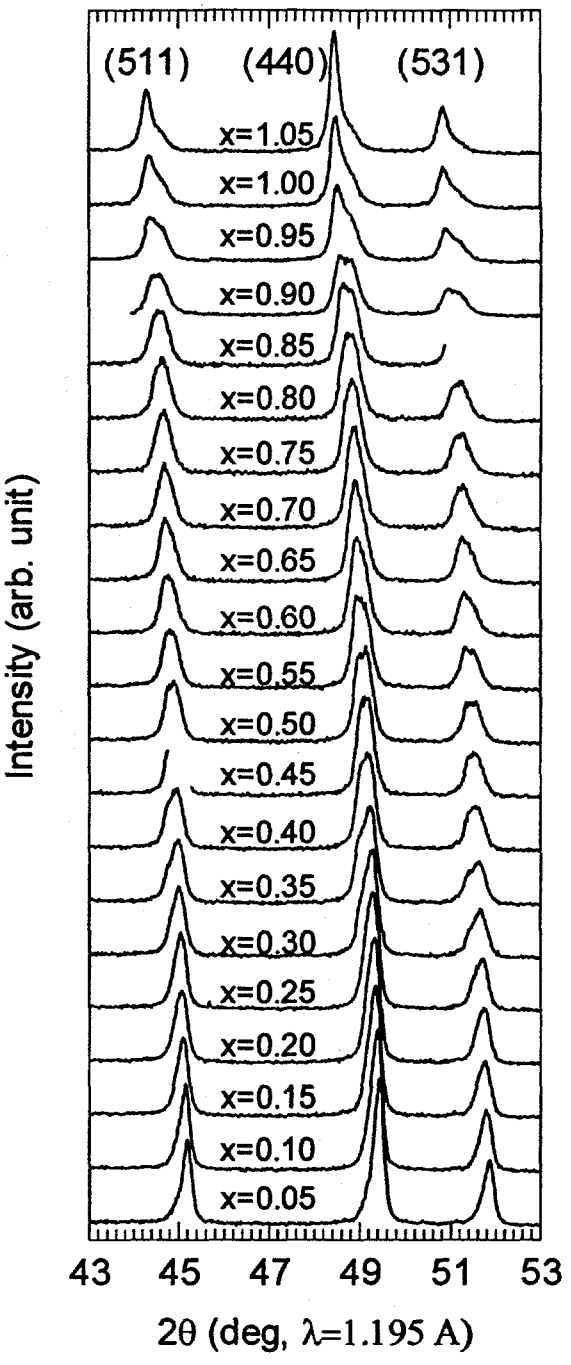

Figure 5. In situ XRD patterns of $Li_xMn_2O_4$ sample A during first discharge with C/10 rate, 32 min for each scan.

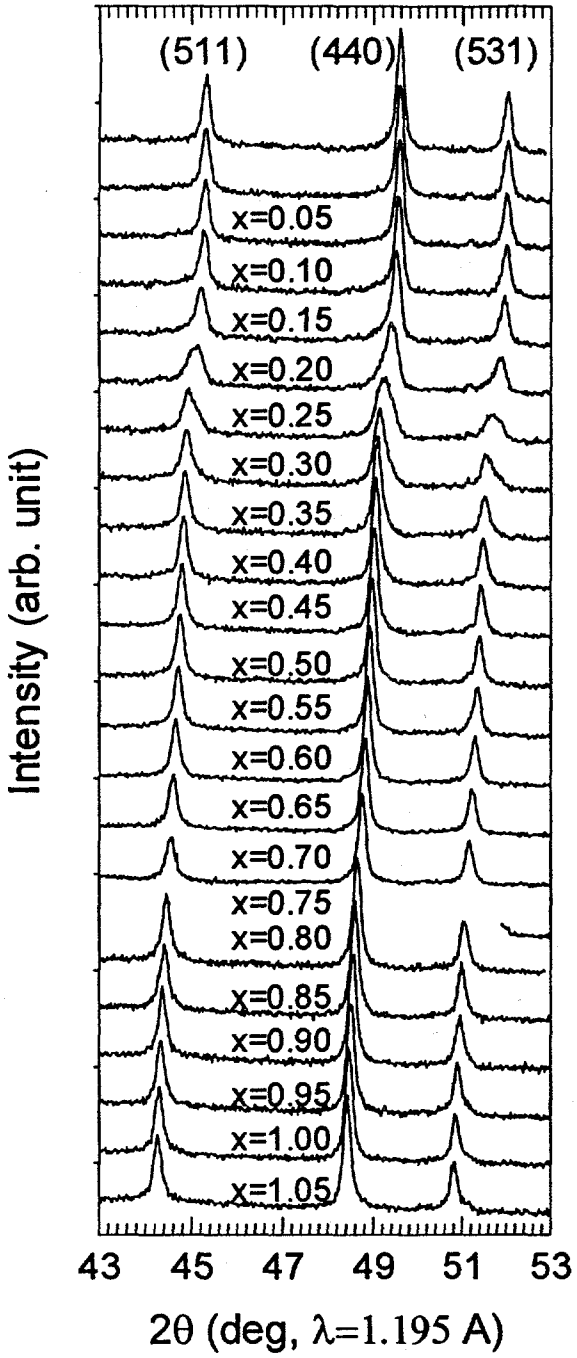

Figure 6. In situ XRD patterns of $Li_xMn_2O_4$ sample B during first charge with C/10 rate, 32 min for each scan.

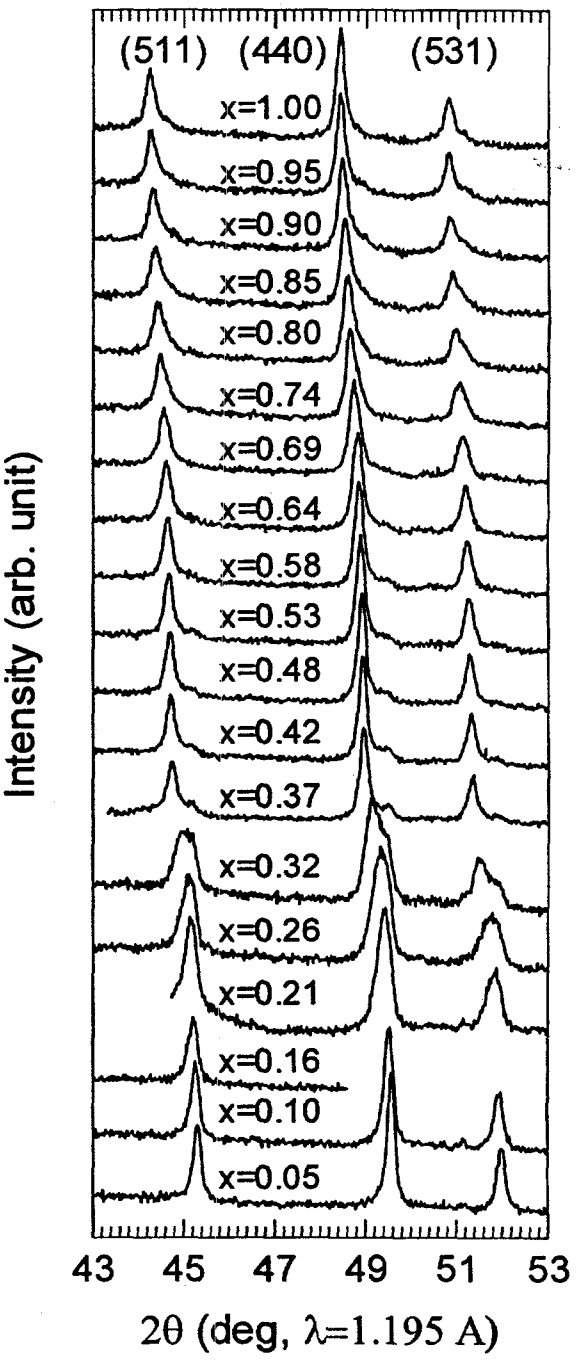

Figure 7. In situ XRD patterns of $Li_xMn_2O_4$ sample B during first discharge with C/10 rate, 32 min for each scan.